Substorm Classification with the WINDMI Model

W. Horton

The University of Texas at Austin, Austin, TX 78712

R.S. Weigel

NRC at NASA/GSFC, Greenbelt, MD 20771

D. Vassiliadis

USRA at NASA/GSFC, Greenbelt, MD 20771

I. Doxas

Department of Physics, University of Colorado, Boulder, Colorado 80309

Abstract

The results of a genetic algorithm optimization of the WINDMI model using a substorm data set are presented. A key result obtained from a computational search for convergence of the prediction over the database is the finding that there are three distinct types of VB_s-AL wave forms. Type I and III substorms are given by the internally-triggered WINDMI model. The WINDMI analysis identifies an additional type of event, called a type II substorm, that requires an external trigger as in the northward turning of the IMF model of Lyons (1995). Intrinsic database uncertainties in the relative timing between the ground based AL electrojet signal and the arrival time at the magnetopause of the IMF data measured by spacecraft in the solar wind prevent a sharp division between type I and II events. Within these timing limitations we find that the fraction of events is roughly 40% type I, 40% type II, and 20% type III.

Institute for Fusion Studies Report No. 945
April 18, 2002

I. INTRODUCTION

In view of the success of the low-order description of magnetospheric dynamics which uses a truncated description of the energy transfer process during a substorm, it is desirable to have a reliable method for optimizing such models over a large historical data set. Two such models are the Faraday loop model (Klimas *et al.*, 1994) and WINDMI (Horton and Doxas, 1996, 1998). These physics based models, in contrast to filter based models which are also used to predict substorm activity, are more difficult to optimize because they can exhibit properties of self organization and bifurcations which can cause a high density of local minima in the error landscape, thus requiring a global search method. For filter based models, including local-linear (Vassiliadis *et al.*, 1994) and neural network (Weigel *et al.*, 1999) filters, the optimization is more straightforward. In the case of linear filter models, a matrix inversion technique exists, which provides the desired minimum error (Box and Jenkins, 1976) For neural network models, a standard back propagation minimization algorithm can be used (Bishop, 1995).

In this work we report on the determination of the optimum parameters of the low order physics model WINDMI which describes the relationship between the energy storage and unloading in the magnetosphere during a substorm. The model contains a concise description of the internal trigger mechanism that occurs from the near-Earth neutral line model. The model appears consistent with the dynamics observed in the global MHD simulations. These internally-triggered unloading events are called type I substorms giving the globally-correlated magnetospheric signatures widely recognized to account for many substorm characteristics (Baker *et al.*, 1999). A type I substorm from the database analyzed here is shown in Fig. 1. In Fig. 1 and the following figures, the solar wind input voltage $V_{\rm SW}$ is shown by the black line, the geomagnetic lower auroral index AL (from ground based magnetometers) is shown in the grey line and the model prediction for AL from $V_{\rm SW}(t)$ is shown in the dot-dash line. The predicted AL follows from $V_{\rm SW}(t)$ by integration of a system of 6 ordinary differential equations given in the next section.

Previous evaluations of this model done in the context of individual substorms showed good performance of the model and qualitative agreement with the 30 hr, slowly rotating large IMF magnetic cloud event (Farrugia *et al.*, 1993) evaluated by Horton *et al.* (1998). In that analysis, the minimization was done by perturbing the base line parameters from

their mean values on an individual substorm. The baseline values of the physics parameter vector $\boldsymbol{P} = (L, M, C, \Sigma, \Omega, u_o, I_c, \alpha, \tau_{||}, \tau_E, L_1, C_1, \Sigma_I, \beta)$ were calculated by Horton and Doxas (1996, 1998) using standard magnetospheric physics models.

With an internal geotail trigger for unloading the WINDMI model based on causality with energy– and charge–conserving power transfer functions yields a precise sequence of events. Thus, it can be used to distinguish between internally-triggered and solar wind-triggered substorms. We have found this discrimination property to be clear and thus useful for identifying the northward turning events.

A second useful property of WINDMI is that it provides a systematic method through comparison of minimum error residuals for testing contributions to the model of higher order physical effects. An additional effect, such as inclusion of the region 2 current loops, can be tested against a database to determine if there is a statistically significant effect on the performance of the model. The evaluation consists of posing the question as to how low the error metric measuring the difference between the predicted $\widehat{AL}$ and the measured AL can be driven for the physics parameters within the standard range of acceptable values. The first modification considered was the inclusion of ionospheric conductivity enhancement due to electron precipitation. The ionospheric conductivity enhancement is based on the relation between the precipitating electron energy flux Φ_E and height integrated Hall and Pederson conductivity as given by Robinson *et al.* (1988). The second modification to the model is the inclusion of an energy coupling to nightside region 2 currents based on the model described by Siscoe (1982). Both of these effects, however, result in minor changes compared to the northward turning events that are the focus of the present study.

II. MODEL DESCRIPTION

We start with the reference model of WINDMI as developed in Horton and Doxas (1996,1998) which conserves charge and energy and describes the causal energy transfer processes in the coupled magnetosphere-ionosphere during substorms. The mathematical expression of the model is given in Eqs. (1)-(6) and an energy flow diagram of the multiple energy pathways is given in Horton *et al.* (1999). The model describes six distinct (and comparable) energy components with six pairs of energy transfer terms. The driven-damped

nonlinear system of six ordinary differential equations (ODEs) is

$$L\frac{dI}{dt} = V_{\rm sw} - V + M\frac{dI_1}{dt} \tag{1}$$

$$C\frac{dV}{dt} = I - I_1 - \alpha P^{1/2} - \Sigma V \tag{2}$$

$$\frac{3}{2}\frac{dP}{dt} = \Sigma\frac{V^2}{\Omega} - u_0 K_{\|}^{1/2}\Theta(I - I_c)P - \frac{P}{\tau_E} \tag{3}$$

$$\frac{dK_{\|}}{dt} = \alpha P^{1/2}V - \frac{K_{\|}}{\tau_{\|}} \tag{4}$$

$$L_1\frac{dI_1}{dt} = V - V_1 + M\frac{dI}{dt} \tag{5}$$

$$C_1\frac{dV_1}{dt} = I_1 - \Sigma_I V_1. \tag{6}$$

The conservation laws for the coupling terms are fundamental properties of the mathematical physics most clearly expressed through algebraic topology (Lefschetz and Solomon, 1975) and (Bamber and Sternberg, 1990).

Equation (1) and (2) describe the evolution of the cross tail potential $V = E_y L_y$ and cross tail current I given the solar-wind driving potential $V_{\rm sw} = \beta v_x B_s L_y$ where the factor β represents the efficiency with which the solar-wind voltage is translated to a cross-tail potential drop. The system of Eqs. (1)-(6) provide a faithful prediction of the standard type I isolated substorm as shown in Horton *et al.* (1999) and earlier works. Figure 2 shows a good example with a sharp unloading that is described well in the top panel with WINDMI. For comparison an optimized LRC filter is shown in the bottom panel to miss the surge of the AL index. The error measure called the average relative variance ARV drops from 0.45 to 0.12 when the unloading is captured. Some substorms, called type III events, are described without the unloading event being triggered.

A careful case by case examination of the phase of region 1 current increase with respect to the change in the convection electric field shows that there is a large class of events (approximately 40%) which the standard WINDMI model, with an internal trigger, cannot reproduce. The model can reproduce these events, however, if an external IMF-Bz-based trigger is added. We call these externally triggered events type-II substorms. An example for the type II substorm is shown in Fig. 3 where we see that there is first a sharp drop in the convection electric field $E_y = V/L_y$ and then an increase in the westward electrojet currents. The $I_1 - V$ phase diagrams for the internal trigger model always have the reverse time sequence of the two signals from that sequence expected by the Kirchhoffian structure

of the WINDMI equations. Therefore, we conclude that the type II events must be triggered by an abrupt drop of the convection electric field. This drop of the convection electric field is a straightforward consequence of an abrupt northward turning of the IMF. This is the scenario envisioned by Lyons (1995) and used by Blanchard *et al.* (2000). Before using the genetic algorithm (GA) minimization technique it was thought that these anomolous substorms were not captured by WINDMI because the ARV minimization technique was stuck in a local minimum. After making long runs (5-10 hrs. with 1000 initial population vectors) with the GA method we are confident that there are a set of events for which an external trigger mechanism is essential.

The WINDMI model goes beyond the linear circuit based models. These represent the basic interaction between the geotail current loop I and nightside region-1 current loops I_1 through the mutual inductance M. In addition WINDMI includes the plasma physics of the internal trigger for unloading plasma pressure through parallel mass flows on newly opened magnetic field lines. The pressure unloading switch describes unloading from the bifurcation of the magnetic field that occurs when the cross-tail current (or the current density $j_y(t) = I(t)/L_x L_z$) reaches a critical level, I_c in Eq. (3). The dawn-to-dusk plasma current is the sum of the pressure gradient current $I_{ps} \propto P^{1/2}$ and the collisionless viscous stress driven current $I_{\rm vis} = \int j_y dxdz = \int dxdz(\hat{\boldsymbol{y}} \cdot \boldsymbol{B} \times \nabla \cdot \boldsymbol{\pi}/B^2) \propto \Sigma V$ driven by plasma convection through the divergence of the ion off-diagonal momentum stress tensor $\boldsymbol{\pi}$ (Horton and Doxas, 1996). The closure of the I_1 current loop subtracts from these currents flowing from dusk-to-dawn in regions obtained by mapping the auroral field lines to the geotail.

The reference model includes an explicit magnetosphere-ionosphere coupling given by Eqs. (5) and (6) These two equations describe the inductive coupling between the lobe current and field aligned region 1 currents. This is in contrast to simplified models which assume that the magnetic field lines connecting the magnetosphere to the ionosphere are equipotentials so that the magnetospheric and ionospheric electric fields are proportional and determined by a mapping factor (Weimer, 1994).

The set of dynamical variables is $\boldsymbol{x} = (I, V, P, K, I_1, V_1)$, and the 14 parameters, which will be taken as constant in first order approximation, are given by $\boldsymbol{P} = (L, M, C, \Sigma, \Omega, u_o, I_c, \alpha, \tau_{||}, \tau_E, L_1, C_1, \Sigma_I, \beta)$.

In this work we use the genetic algorithm for finding the optimal the error minimization of WINDMI with respect to the parameter set $\boldsymbol{P}$ with minimal difference between the

model AL and the database AL. The values of the parameters are restricted since they are based on calculations of magnetospheric quantities such as the lobe inductance, the plasma capacitance and conductance. A direct physics estimate of the lobe inductance and the plasma sheet capacitance is taken from Horton and Doxas (1996, 1998) and Doxas and Horton (1999). In Table 1 we list estimated values of all magnetospheric-ionospheric parameters in the base model. These estimates have been derived and calculated previously by Horton and Doxas (1996, 1998). The most intricate calculation involves the average CPS conductance Σ where the chaotic motion of the ions leads to an anomolous conductivity, see Horton and Tajima (1991).

III. OPTIMIZATION METHODS

Here we are optimizing the parameters of a nonlinear set of differential equations which have a wide variety of possible dynamics including limit cycles, chaotic attractors and fixed points (Smith *et al.*, 2000; Horton *et al.*, 2001). Since this type of minimization which involves optimizing the parameters of a nonlinear set of differential equations does not have a standard solution we have tried three approaches (random grid search, gradient descent, genetic algorithms) and find the best results with the genetic algorithm. The random grid search is numerically prohibitive because the time required scales with N_p^N where N is the number of grid points per parameter, and N_p is the number of parameters. Also the gradient descent type algorithms have difficulty when encountering local minima.

We minimize the error function $ARV = ARV(\boldsymbol{P})$ where the parameter vector $\boldsymbol{P}$ has elements which are bounded by estimates of the maximum and minimum estimates defined in $\boldsymbol{P}_{\max} = (\mathcal{L}_{\max}, ..., \Sigma_{I_{\max}})$ and $\boldsymbol{P}_{\min} = (\mathcal{L}_{\min}, ..., \Sigma_{I_{\min}})$.

The minimization procedure then follows the standard genetic algorithm technique in which a population of parameter vectors $\boldsymbol{P}$ are tested, sorted according to ARV, and then split and re-combined with other parameter vectors (Vose, 1999). In this problem an initial set of 1000 parameter vectors were used.

IV. OPTIMIZATION RESULTS

We show the performance of the base WINDMI model on several intervals of the Blanchard-McPherron (1993) substorm database. First we note that certain substorm intervals have a very low error ($ARV = 0.12$). For example, consider the following result of minimization on the Blanchard-McPherron interval as shown in Fig. 1. An observation which is made from considering the intervals with the lowest error is that the intervals which are most easily predicted tend to have the classic substorm AL structure with respect to the southward turning of the IMF.

From the distribution of ARVs for the substorms in the two data sets, we see that there are many intervals that are adequately predicted by the WINDMI model with an internal trigger (86 events with $ARV < 1.0$). There are two other groups for which the model does poorly: Group 1 with 24 events with $1.0 \leq ARV \leq 2.0$ and 7 intervals in Group 2 with $ARV > 2.0$.

The WINDMI validation problem was thought to be that the minimization procedure was not able to find the correct parameter values. After a thorough search using the genetic algorithm method it was concluded through a careful case by case examination of the phase of the region 1 current increase with respect to the phase of the convection electric field that there are the type II events that are not described by the WINDMI model with an internal trigger. A type II substorm is shown in Fig. 3 where we see that there is *first* a sharp decrease in the convection electric field $E_y = V/L_y$ *followed by* an increase in the westward electrojet current as measured by the AL index. The I_1-V phase diagrams have the reverse time ordering for an internally triggered event. Therefore, we conclude that these type II events are triggered by an abrupt drop of the convection electric field. This scenario then conforms to the northward turning substorm trigger scenario of Lyons (1995) and Rostoker (1983).

In Fig. 3 the northward turning solar wind triggered event is shown. When the northward turning is fast, the Earth convection of hot ion plasma stops, a strong dawn-dusk asymmetry occurs as described by Lyons (1995) and there is an abrupt dipolarization of the near-Earth field. In the bottom panel of Fig. 3 an external northward turning IMF trigger was added following the description of Blanchard *et al.* (2000). After eliminating the weak type III substorms that are well fit by WINDMI, we find that approximately one-half of

the Blanchard-McPherron database is of type II. This is a strong revision of the classical substorm picture of a near-Earth neutral line being the first event in the substorm scenario. Lyons (1996) argues that perhaps even a majority of the substorm events are of the type II.

Finally, other substorms are shown in Fig. 4 where only the directly-driven response is used by WINDMI without triggering. These substorms agree with the Akasofu (1980) picture. In general the type III substorms are weaker in AL for this database.

The wide distributions of the parameter histograms and increase in ARV when using the mean parameter set, $\overline{\boldsymbol{P}}$ is similar to that encountered when fitting the parameters for linear filter models of substorms. In the linear filter case, the ARV increased from 0.29 to 0.53 when the mean value of the parameters was used (Blanchard and McPherron, 1993). This is a manifestation of either the intrinsic unpredictability of the M-I system, solar wind noise (Goode *et al.*, 2001), or effects not included in the modeling.

V. DISCUSSION AND CONCLUSIONS

This work has described the results of using the genetic algorithm for deriving the optimal parameters for the WINDMI model with an internal plasma loading-unloading switch based on the near-Earth neutral line model. After extensive minimization studies we find that there is a significant set ($\sim 40\%$) of substorm events for which convergence of the internal trigger model and the data are not achieved. After eliminating the possibility of numerous other physical effects (Weigel, 2000) that might account for this result, we conclude that an external solar-wind-based trigger mechanism from the abrupt northward turning of the IMF is required. The results described here give a digital method of classifying substorm signals into three broad physical categories. With the quantitative, physical model WINDMI this division of the types of substorms is firmly established. An external solar-wind-based trigger is required for a large fraction of the substorms.

The key point here is that by having a physics modeling, there is a definite causal time ordered sequence of events for the internally triggered unloading events. This is in contrast to neural networks, for example, that have no physical constraints. From a histogram of ARVs, we see that that approximately 40% of the events are of the classical unloading type and 40% are type II events where the phase relations are reversed. The precise division between the two types of unloading events will remain uncertain until better methods are found for timing

the arrival of the solar wind to the Earth's magnetopause. Weimer (1994) points out there are uncertainties in this timing analysis that are as large as 10min. There are weaker events that are directly driven with out setting off an unloading event according to the optimized WINDMI model. This finding is consistent with the long standing controversy between the directly driven substorm and the loading-unloading substorm scenarios. According to the WINDMI analysis both these type I and type III events are required by the databases.

Weigel (2000) has explored the impact of adding several well known physical processes left out of the WINDMI model. The analysis shows that these changes do not effect the classifications presented here. The conclusion from these upgrades was that there are quantitative reductions of the ARV at the 5% -10% level, but no change in the overall profile of the correlated input-output signals.

VI. ACKNOWLEDGMENTS

The work was supported by the NSF Grant No. ATM-9907637 and NASA Grant NAG5-6198. Computing resources were provided by the Texas Advanced Computing Center (TACC).

References

Akasofu, S.-I., The solar-wind magnetosphere energy coupling and magnetospheric disturbances, *Planet. Space Sci., 28*, 295, 1980.

Baker, D.N., T.I. Pulkkinen, J. Büchner, and A.J. Klimas, Substorms: A global instability of the magnetosphere-ionosphere system, *J. Geophys. Res., 104*, 14,601-14,611, 1999.

Bamber, P., and Sternberg, S., A course in Mathematics for Students of Physics, Cambridge University Press, Cambridge, MA, 1990, vol. 2, pp. 407-474.

Bishop, C. M., *Neural networks for pattern recognition*, Oxford University Press, 1995.

Blanchard, G. T., and R. L. McPherron, A bimodal representation of the response function relating the solar wind electric field to the AL index, *Adv. Space Res., 13*, 71, 1993.

Blanchard, G.T., L.R. Lyons, and J. Spann, Predictions of substorms following northward turnings of the interplanetary magnetic field, *J. Geophys. Res., 105*, 375, 2000.

Box, G. E. P., and G. M Jenkins, *Time Series Analysis: Forecasting and Control*, San Francisco, Holden-Day, 1976.

Doxas, I., and W. Horton, Magnetospheric dynamics from a low-dimensional nonlinear dynamics model, *Phys. Plasmas, 6*, 3, 1-7, 1999.

Farrugia, C. J., M. P. Freeman, L. F. Burlaga, R. P. Lepping, and K. Takahashi, The earth's magnetosphere under continued forcing: Substorm activity during the passage of an interplanetary magnetic cloud, *J. Geophys. Res., 98*, 7657, 1993.

Goode, B., I. Doxas, J. R. Cary and W. Horton, Differentiating between colored random noise and deterministic chaos with the root mean squared deviation, *J. Geophys. Res., 106*, 21,277 2001.

Horton, W., and T. Tajima, Transport from Chaotic Orbits in the Geomagnetic Tail, Geophys. *Res. Lett., 18*, 1583-1586,1991, and a recent extension by R.

Numata and Z. Yoshida, *Phys. Rev. Lett.*, 2002.

W. Horton and I. Doxas, A low dimensional dynamical model for the solar wind driven geotail–ionosphere system, *J. Geophys. Res., 101*, 27223, 1996.

Horton, W., and I. Doxas, A low-dimensional dynamical model for the solar wind driven geotail-ionosphere system, *J. Geophys. Res., 103*, A3, 4561, 1998.

Horton, W., M. Pekker, and I. Doxas, Magnetic energy storage and the nightside magnetosphere-ionosphere coupling, *Geophys. Res. Lett., 25*, 4083, 1998.

Horton, W., J. P. Smith, R. Weigel, C. Crabtree, I. Doxas, B. Goode, and J. Cary, The solar-wind driven magnetosphere-ionosphere as a complex dynamical system, *Phys. Plasmas, 6*, 11, 1-7, 1999.

Horton, W., R.S. Weigel, and J.C. Sprott, Chaos and the Limits of Predictability for the Solar-Wind-Driven Magnetospheric-ionospheric system, *Phys. Plasmas, 2946*, 2001.

Klimas, A. J., D. N. Baker, D. Vassiliadis, and D. A. Roberts, Substorm recurrence during steady and variable solar wind driving: Evidence for a normal mode in the unloading dynamics of the magnetosphere, *J. Geophys. Res., 99*, A8, 14855, 1994.

Lefschetz and Solomon, "Applied Mathematical Sciences," in *Applications of Algebraic Topology : Graphs and Networks: the Picard-Lefschetz Theory and Feynman Integrals*, Springer-Verlag, New York, 1975, v. 16, pp. 1884-1972.

Lyons, L. R., A new theory for magnetospheric substorms, *J. Geophys. Res., 100*, 19,069, 1995.

Lyons, L. R., Substorms: Fundamental observational feautres, distinction from other disturbances, and external triggering, *J. Geophys. Res., 101* 13,011-13,025, 1996.

Robinson, R. M., R. R. Vondrak, K. Miller, T. Dabbs, and D. Hardy, On calculating ionospheric conductances from the flux and energy of precipitating electrons, *J. Geophys. Res., 92*, 2265-2569, 1988.

Rostoker, G., Triggering of expansion phase intensifications of magnetospheric

substorms by northward turnings of the interplanetary magnetic field, *J. Geophys. Res., 88*, 6981, 1983.

Siscoe, G. L., Energy coupling between regions 1 and 2 Birkeland current systems, *J. Geophys. Res., 87*, A7, 5124, 1982.

Smith, J. P., J.-L. Thiffeault, and W. Horton, Dynamical range of the WINDMI model: An exploration of possible magnetospheric plasma states, *J. Geophys. Res., 105*, A6, 12,983, 2000.

Vassiliadis, D., A. J. Klimas, D. N. Baker, and D. A. Roberts, A description of solar wind-magnetosphere coupling based on nonlinear filters, *J. Geophys. Res., 99*, 3495, 1994.

Vose, M. D., *The Simple Genetic Algorithm: Foundations and Theory*, Cambridge Univ. Press, Cambridge, MA, 1999.

Weigel, R. S., W. Horton, T. Tajima, and T. Detman, Forecasting auroral electrojet activity from solar wind input with neural networks, *Geophys. Res. Lett., 26*, 1353, 1999.

Weigel, R.S., Prediction and modeling of magnetospheric substorms, Ph.D. thesis, THe University of Texas at Austin, 2000.

Weimer, D. R., Substorm time constants, *J. Geophys. Res., 99*, A6, 11005, 1994 and AGU, 2001.

Parameter	Est. Value
L (H)	40.0
M (H)	1.0
C (F)	$1.2 \cdot 10^4$
Σ (mho)	40.0
Ω (m^3)	$1.6 \cdot 10^{24}$
u_o ($J^{-1/2}s^{-1}$)	$6.0 \cdot 10^{-11}$
I_c (A)	$2.2 \cdot 10^7$
α ($A \cdot Pa^{-1/2}$)	$1.0 \cdot 10^{12}$
$\tau_{\|\|}$ (s)	$1.0 \cdot 10^3$
τ_E (s)	$1.0 \cdot 10^3$
L_1 (H)	12.0
C_1 (F)	$1.0 \cdot 10^3$
Σ_I (mho)	4.0
β_V	0.25

TABLE I: Estimated values of the 14 magnetospheric parameters used in the reference model.

FIGURE CAPTIONS

FIG. 1. A type I substorm example from case 15 of the Blanchard–McPherron dataset. The dark thick line is $V_{\mathrm{sw}} = \beta v_x B_s L_y$, the thick light line is AL, and the dotted line is the response of WINDMI.

FIG. 2. A type I substorm example from the Blanchard–McPherron dataset (case 35: Aug. 18, 1978). Top Panel: The optimized WINDMI system captures the rapid rise in AL that begins at $t = 200$ min. The ARV is 0.12. Bottom panel: The optimized LRC filter prediction is shown to miss the rapid rise in AL which occurs before the rapid reduction in $v_x B_s$. The ARV is 0.45.

FIG. 3. Top Panel: A type II substorm example from the Blanchard–McPherron dataset (case 10: April 4, 1979). The onset which occurs at $t = 65$ min immediately follows a sharp reduction in $v_x B_s$. The dark thick line is $V_{\mathrm{sw}} = \beta v_x B_s L_y$, the thick light line is AL, and the dotted line is the response of WINDMI. The WINDMI response follows the general shape of AL, but the rapid onset phase is not evident. The ARV is 0.30. Bottom Panel: The dotted line is the response of WINDMI with a northward turning trigger initiated at $t = 65$ min. The ARV is 0.06.

FIG. 4. Example of a type III substorm (case 98: Oct. 9, 1978). The AL–$v_x B_s$ response is predicted accurately using the WINDMI model model with no triggering.

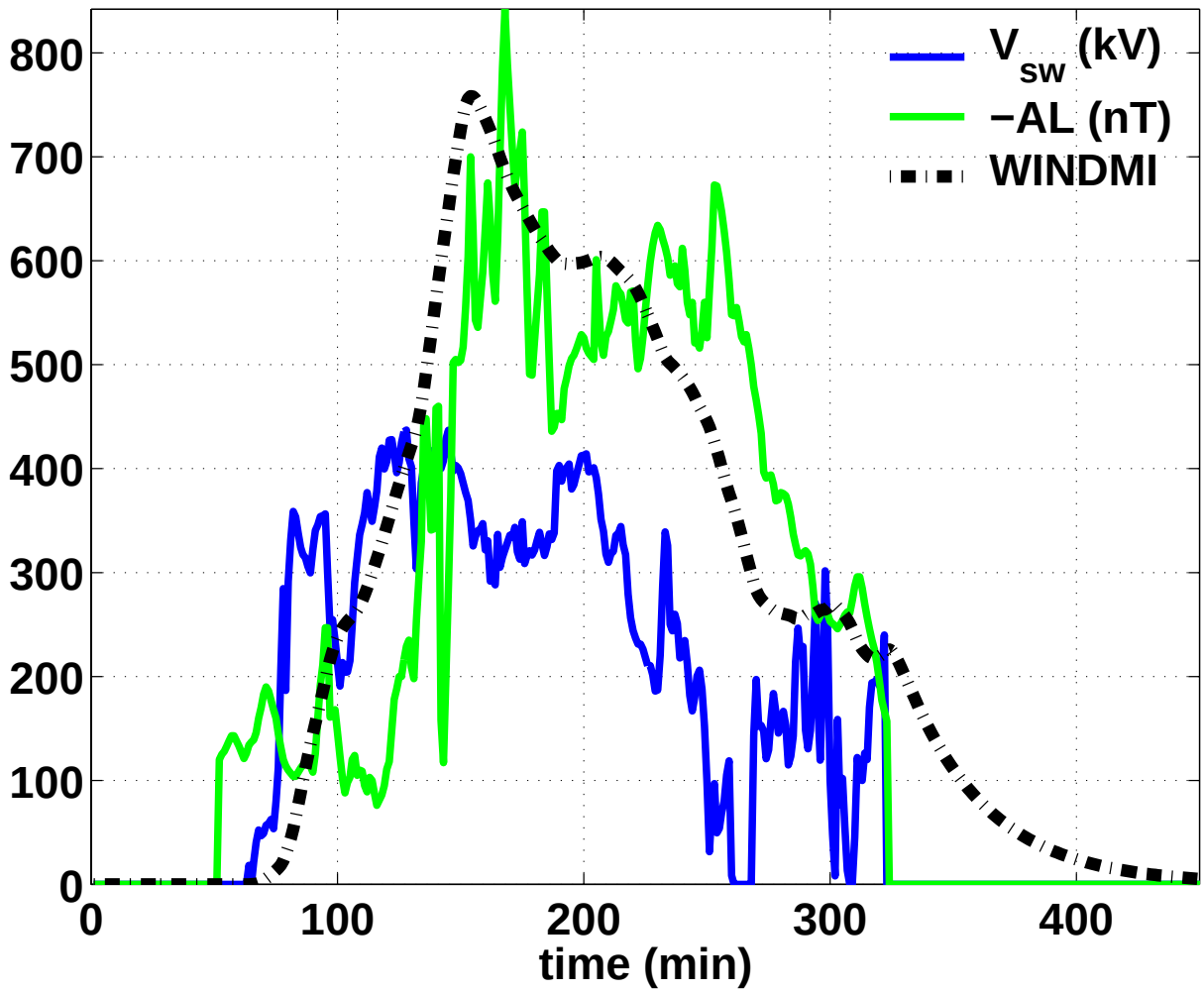
800
700
600
500
400
300
200
100
0
0
100
200
300
400
time (min)
V sw (kV)
−AL (nT)
WINDMI

FIG. 1:

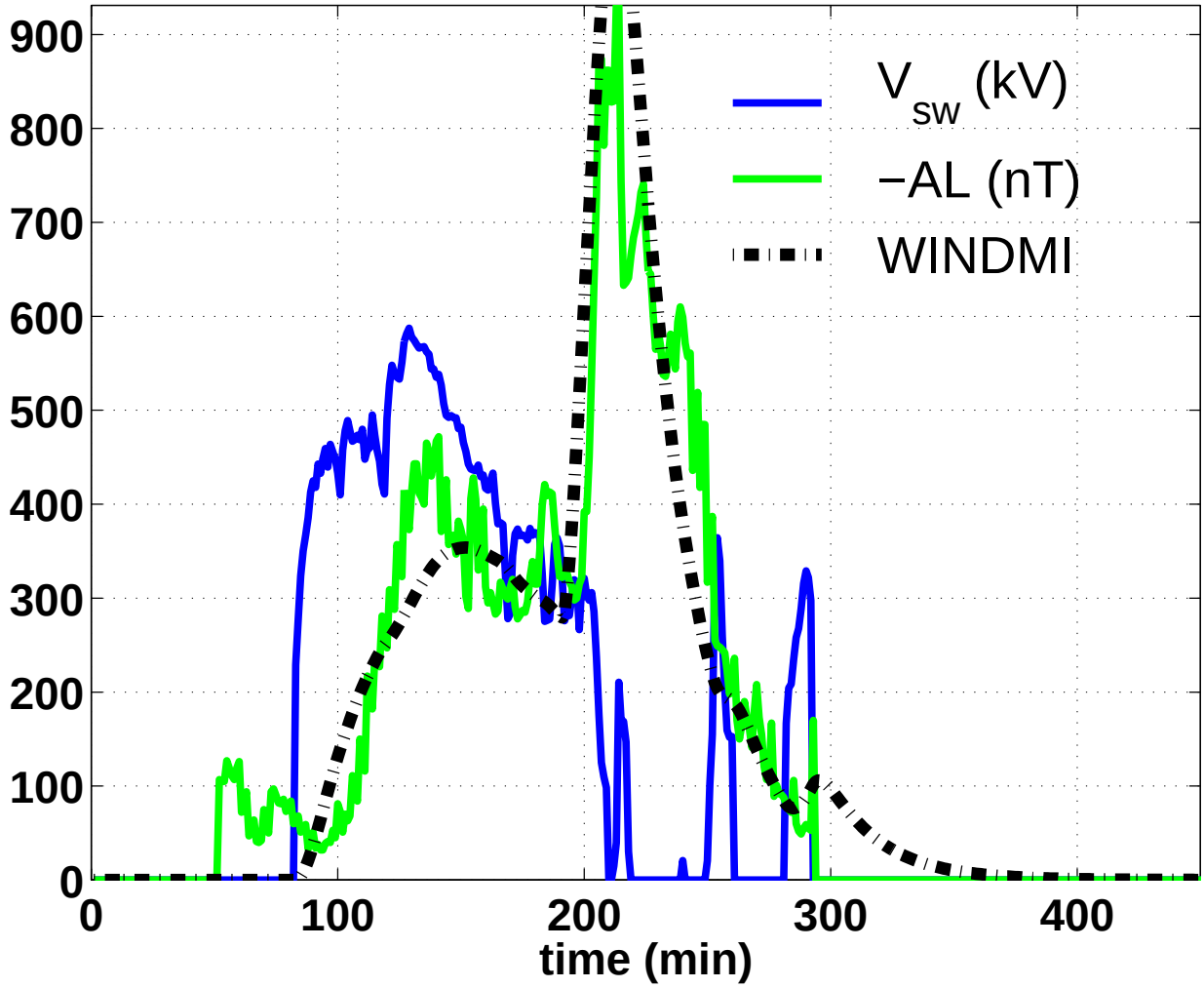
900
800
700
600
500
400
300
200
100
0
0
100
200
300
400
time (min)
V sw (kV)
−AL (nT)
WINDMI

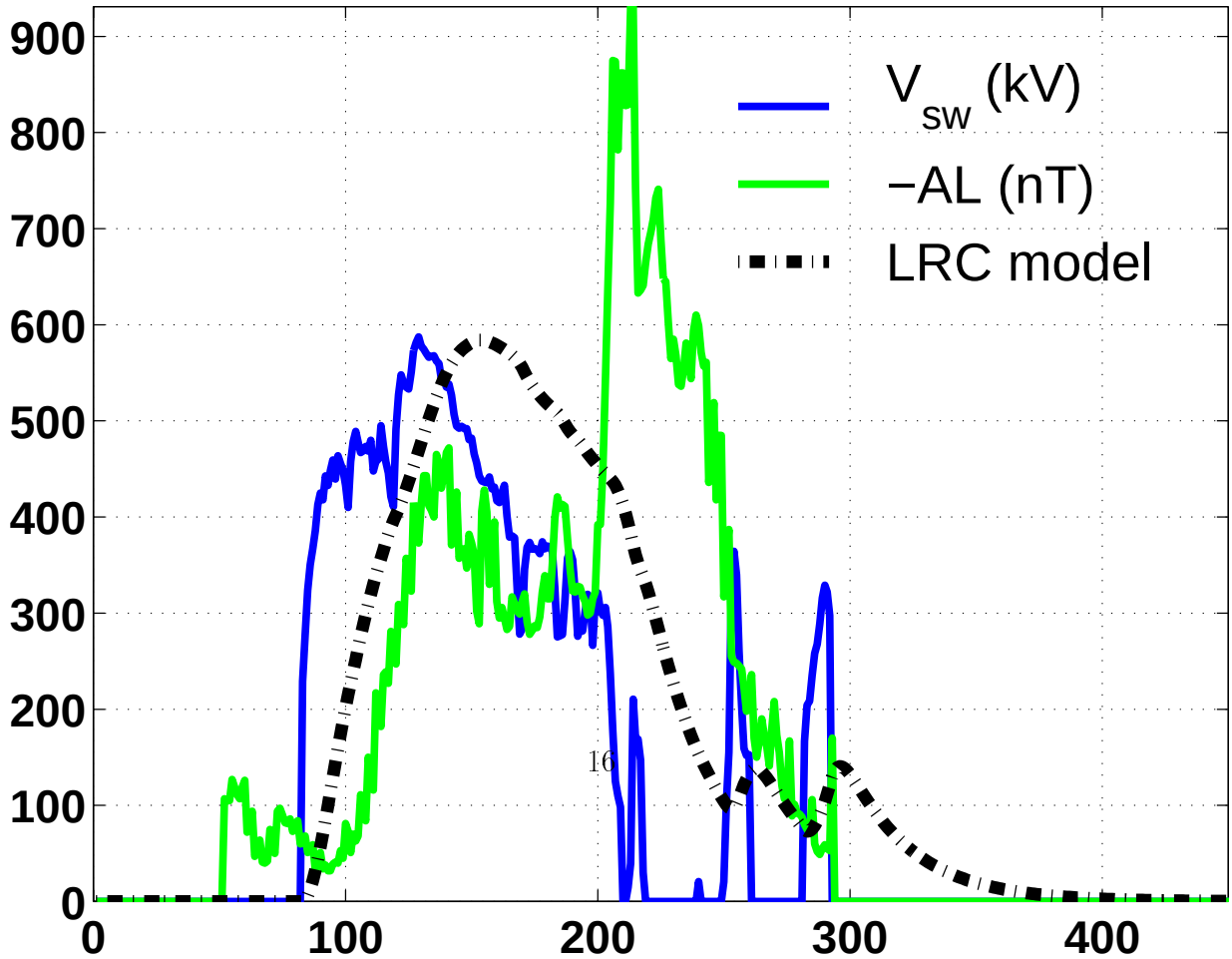
900
800
700
600
500
400
300
200
100
0
0
100
200
300
400
V sw (kV)
−AL (nT)
LRC model

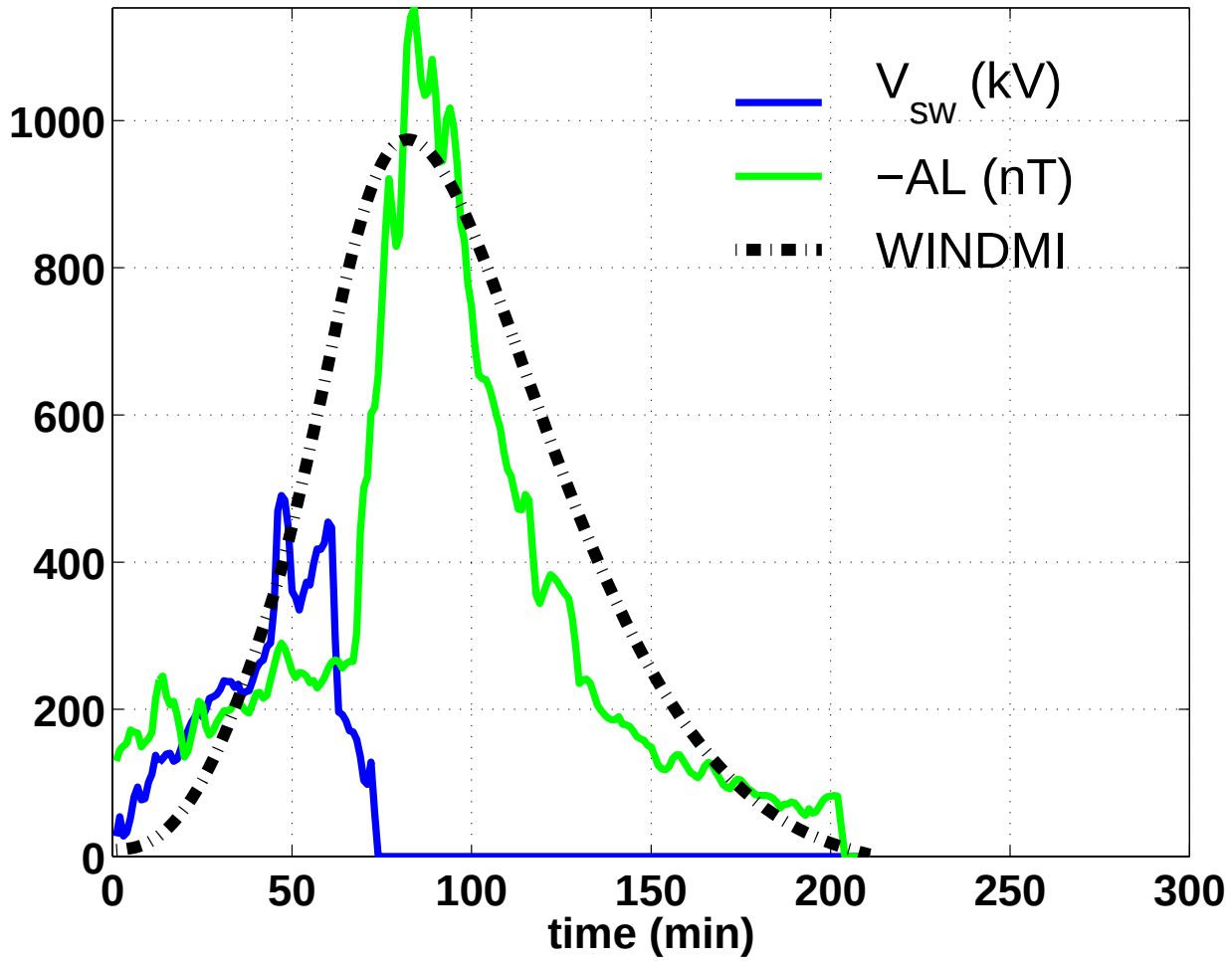
V sw (kV)
−AL (nT)
WINDMI
1000
800
600
400
200
0
0
50
100
150
200
250
300
time (min)

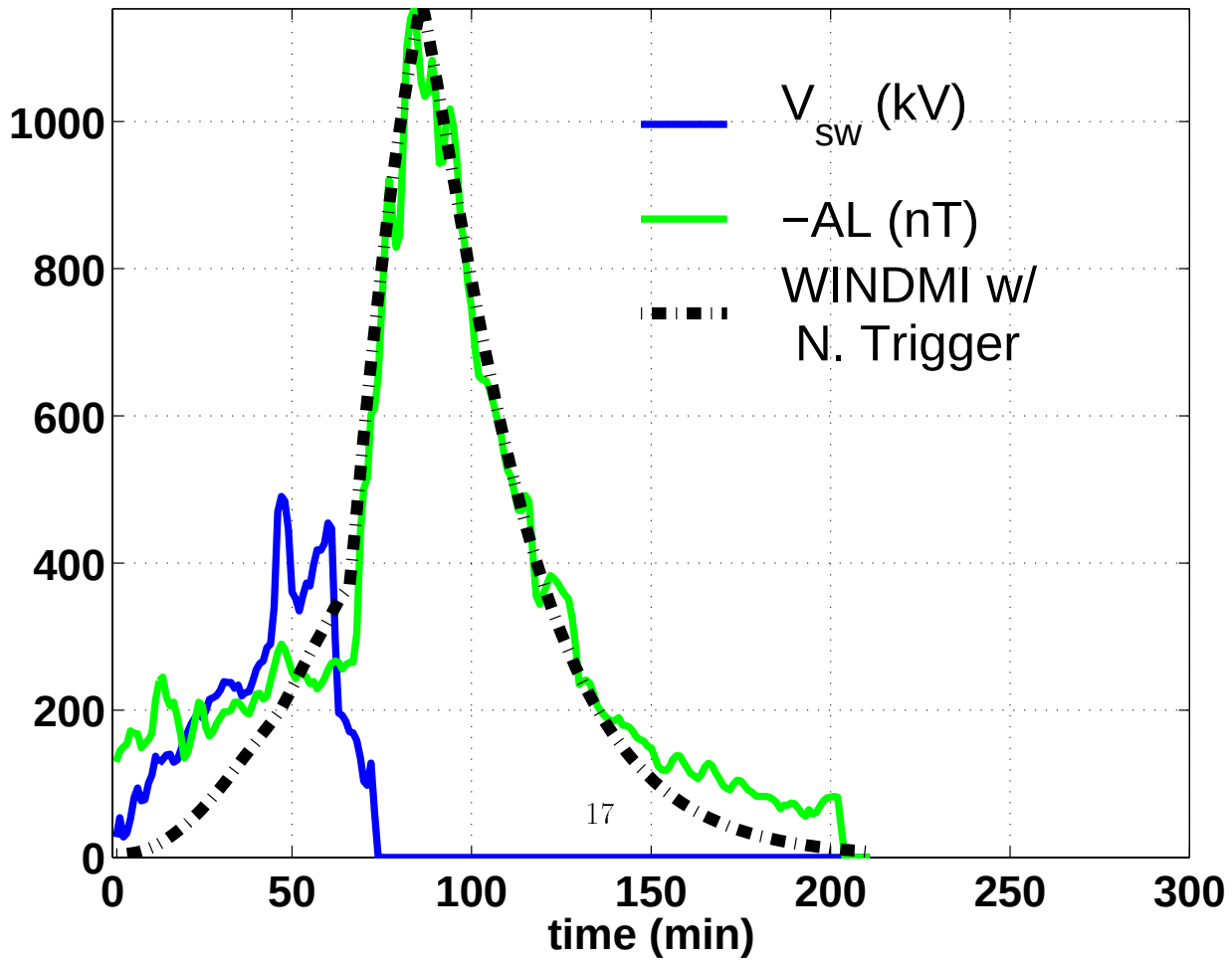
V sw (kV)
−AL (nT)
WINDMI w/
N. Trigger
1000
800
600
400
200
0
0
50
100
150
200
250
300
time (min)

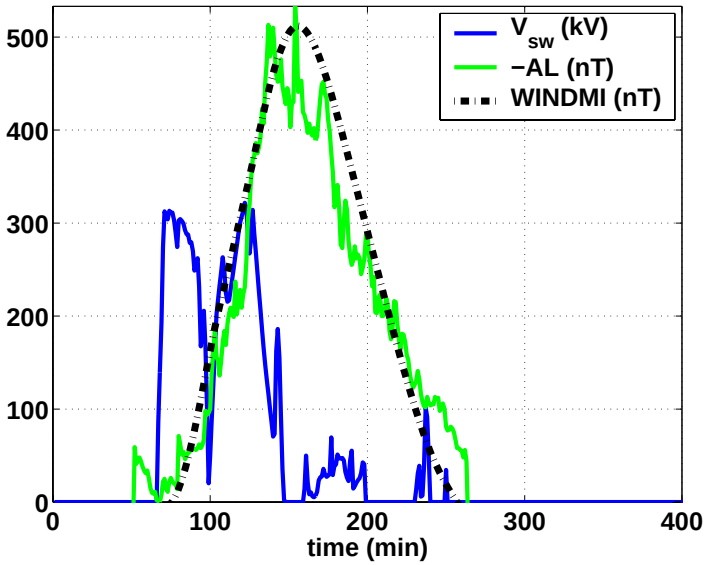
V sw (kV)
−AL (nT)
WINDMI (nT)
500
400
300
200
100
0
0
100
200
300
400
time (min)

FIG. 4: